



# Biosynthesis and Characterization of Silver Nanoparticles Using the Sewage of a Leather Factory in Corn Steep Liquor

Naeimeh Faridi Aghdam<sup>1</sup>, Shahram Moradi<sup>1\*</sup>, Sirous Ebrahimi<sup>2</sup>, Hamed Hamishehkar<sup>3</sup>

## Abstract

**Objectives:** This study aimed to report a simple environmentally compatible method that is economically affordable for the facile biosynthesis of stable silver nanoparticles (AgNPs) in corn steep liquor (CSL) nutrient using the sewage of a leather factory.

**Materials and Methods:** The biosynthesis of AgNPs were done by reduction of AgNO<sub>3</sub> in the sewage of leather factory as a mixed bacterial culture and corn steep liquor under anaerobic condition while protecting from light.

**Results:** The AgNPs were found to have a characteristic absorption peak at 416 nm on the ultraviolet-visible spectrum. Characterization of AgNPs was performed by x-ray diffraction (XRD) and Fourier-transform infrared (FTIR). The scanning electron microscopy (SEM) and transmission electron microscopes (TEM) images showed poly-dispersed spherical stable AgNPs with a maximum diameter of 20 nm. Moreover, the dynamic light scattering (DLS) showed that the average size of AgNPs was 15.57 nm with a zeta potential value of -19.2 mV. The synthesized nanoparticles demonstrated more antibacterial activity in opposition to gram-negative bacteria. The zone of inhibition of biosynthesized AgNPs in 1 mM concentration of AgNO<sub>3</sub> against *Escherichia coli* was equal to that of gentamicin.

**Conclusions:** The interaction of protein residues with AgNPs was identified, supporting that the proteins not only act as a reducing agent but also as a capping. The synthesized AgNPs showed antibacterial activity, providing commercial viability in biomedicine.

**Keywords:** Silver nanoparticles, Biosynthesis, Sewage, Leather factory, Corn steep liquor

## Introduction

Silver nanoparticles (AgNPs) have a diverse range of applications, including catalysis, selective coating, imaging, water treatment, and sterilization process in medical equipment and textiles. Due to their effective antimicrobial properties and low toxicity effect, AgNPs are becoming important nanomaterials for use in consumer products (1-3).

Recently, biogenic AgNPs have shown more antimicrobial activity compared to chemical AgNPs (20 times). The NPs synthesized chemically do not have medical applications due to contamination from precursor chemicals. AgNPs attach to the cell membranes, leading to protein denaturation and cell death (4,5). Silver interacts with protein, which results in forming biomolecular capping around the nanoparticles and more stability of AgNPs. Biomolecular capping improves the antimicrobial activity of AgNPs by better interaction between nanoparticles and microorganisms (6-8).

Different methods have been employed to synthesize NPs with different sizes, stabilities, and performances. The physical and chemical methods have heightened environmentally concerns due to producing dangerous

by-products (9,10). Although these methods afford stable NPs, they are economically expensive (11). So, it is essential that organic sources be employed to synthesize secure and environmentally compatible AgNPs for different applications so that it does not require making use of specific thermodynamic conditions or hazardous materials. This green technology is economically affordable and biocompatible, and it needs a comprehensible scaling up procedure. The synthesis of AgNPs through organic routes (such as bacteria, actinomycetes, yeast, fungi, and plants) has been extensively announced (12,13). The most important advantage of the biological method is that the chemical compositions in the organic sources take a double role: a) reducing agent and b) capping agent.

Bacteria are self-regulated particles that can produce nano-scaled grains (14). In addition, they provide the opportunity to recover useful metals from waste stream because of their unique area (15).

Considering the wide application of AgNPs, it is essential to commercialization (mass production) biogenic AgNPs. Biosynthesis of AgNPs by a pure culture of bacteria in laboratory grade nutrient imposes a high cost of sterilization and feed, which makes it difficult to

Received 7 March 2023, Accepted 10 November 2023, Available online 23 November 2023

<sup>1</sup>Faculty of Chemistry, Islamic Azad University, North Tehran Branch, Tehran, Iran. <sup>2</sup>Biotechnology Research Centre, Faculty of Chemical Engineering, Sahand University of Technology, Tabriz, Iran. <sup>3</sup>Drug Applied Research Center, Tabriz University of Medical Sciences, Tabriz, Iran

\*Corresponding Author: Shahram Moradi, Email: Shm\_moradi@iau-tnb.ac.ir



## Key Messages

- ▶ The biosynthesis of AgNPs by a pure culture of bacteria in laboratory grade nutrient imposes a high cost of sterilization and feed, which makes it difficult to commercialize. To overcome this problem, in the laboratory scale, we selected the sewage of a leather factory as a mixed bacterial culture and CSL as a cost-effective nutrient.

commercialize. To overcome this problem, in this work, we selected the sewage of a leather factory as a mixed bacterial culture and corn steep liquor (CSL) as a cost-effective nutrient. These green routes for fabrication of NPs have gained primacy due to compatibility with environment and reasonable costs compared to previous forms of synthesis.

In this study, the nanoparticles were characterized by ultraviolet-visible (UV-Vis) spectroscopy, X-ray diffraction (XRD), scanning electron microscopy (SEM), transmission electron microscopy (TEM), dynamic light scattering (DLS), zeta potential, and Fourier-transform infrared (FTIR). Also, the antibacterial activity of AgNPs against *Escherichia coli* was investigated using the disk diffusion method.

## Materials and Methods

### Chemicals

CSL was obtained from Glucosan Company (Qazvin, Iran) on separate occasions and stored at 4 °C. The crude CSL was diluted with distilled water (1:20, v/v). Then, the addition of NaOH solution calibrated the pH of the solution to 7.0 (50% w/w). Next, the CSL solution was centrifuged at 9000 rpm for 20 minutes to separate solid materials. Silver nitrate, Muller-Hinton broth, and Muller-Hinton agar were obtained from the Merck Company (Germany).

### Bacterial Strain Growth and Biosynthesis of AgNPs

The mixed bacterial cells were obtained from the sewage of a leather factory (without any treatment) and cultured in CSL medium (COD = 34000 mg/L) at 37 °C with continuous agitation (250 rpm) for 24 hours in screw-capped flasks under aerobic condition. The growth of bacteria was observed by calculating the optical density (OD) at  $\lambda=600$  nm. Silver nanoparticles were prepared by addition of 17 mg of AgNO<sub>3</sub> to 100 mL of bacterial culture and incubated at 37 °C with continuous agitation (250 rpm) under anaerobic condition while protecting from light during the reduction time. Control experiments were done by considering that biomass and heat-killed cells were not added. To separate the AgNPs, the bacterial cells were harvested by centrifugation of reaction mixture (6000 rpm, 15 minutes). Then the supernatant was ultra-centrifuged (100 000 rpm, 20 minutes) to dislodge AgNPs. The obtained AgNPs were rinsed twice with Milli-Q water till the supernatant's conductivity reached below 20  $\mu\text{s}/\text{cm}$ .

## Characterization of Silver Nanoparticles

The optical properties (SPR, shift and the intensity) of the AgNPs were identified by UV-Vis spectrophotometer (UV-2000, Pharmacia, Biotech, England). The crystallization peaks of synthesized AgNPs were scrutinized using powder XRD (Siemens-Germany, 35 kV-30 mA (Cu-K $\alpha$ )). The particle size and surface morphology of AgNPs were analyzed using SEM (KYKY-EM3200, USA) and The NPs' purity was investigated by EDX. To have further authentication for size and morphology of AgNPs, TEM (Zeiss LEO 906, Germany) was operated (200 kV). A droplet of AgNPs was placed on carbon-coated copper grids and its moisture was taken overnight before observation. DLS was operated to evaluate the size distribution of NPs in the medium, and zeta potential (ZP) analysis was used to determine the stability (Zetasizer Ver. 6.20, Malvern Instruments, England). The functional groups of biomolecules which are responsible for the reduction and capping of the AgNPs were analyzed by FT-IR spectroscopy (BRUKER, USA).

### Antibacterial Study of AgNPs

Disk diffusion method was performed to study the antibacterial activity of AgNPs which had been synthesized in extracellular against cancer-inducing gram-negative bacteria strains (*E. coli*) on Muller-Hinton agar plates (16). The blank disks from the Merck Company were considered. To determine the bactericidal effect, each standard disk was impregnated with 2 mL of different fresh biosynthesized AgNPs using various AgNO<sub>3</sub> concentrations (0.25, 0.5 and 1 mM) in the mixed bed culture of bacteria. By dilution, the *E. coli* bacteria required for inoculation were cultured overnight in Muller-Hinton broth. Bacteria at a 0.5 McFarland standard were cultured on Müller Hinton agar plate and then the discs were placed on those plates. After incubation at 37 °C for 24 hours, susceptibility of the bacteria was evaluated by measuring the zones of inhibition. The assay was applied in triplicate.

## Results

### UV-Visible Spectral Analysis of AgNPs

The biosynthesized AgNPs using mixed bed bacteria in CSL were approved by visually monitoring the well-known color alteration from transparent pale yellow to dark brown (9,17).

The absorption spectrum (Figure 1) of dark brown AgNPs expressed a surface plasmon absorption band (SPR) at approximately 416 nm. Control experiments, which lacked biomass and heat-killed cells, did not show any brown color, proving that color alteration was due to live biomass.

### Crystalline Structure of AgNPs

The XRD analysis of the prepared AgNPs illustrated the characteristic peaks attributed to silver metal confirming the existence of crystalline phases in structure of

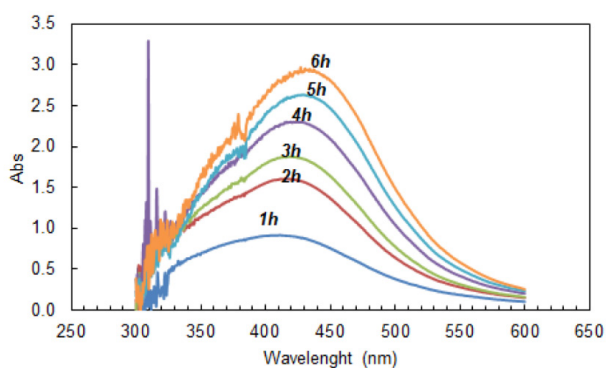


**Figure 1.** UV-Vis spectra recorded as a function of reaction time of silver nitrate with the bacterial cell culture in CSL.

nanoparticles (Figure 2). The diffractive intensities were recorded over  $2\theta$  ranges from  $20^\circ$  to  $90^\circ$ . Four strong peaks at  $38.01^\circ$ ,  $45.47^\circ$ ,  $66.27^\circ$  and  $75.24^\circ$  correspond to the (111), (200), (220), and (311) planes of metallic Ag crystalline lattice (JCPDS No. 04-0783), respectively, which can be interpreted to the face centered cubic (FCC) lattice structure of crystalline AgNPs (18). Vijayan et al synthesized AgNPs using seaweed and reported the same structure of AgNPs (19). Other unallocated peaks might be related to the bio-organic molecules which are part of the reaction mixture utilized for reduction and stabilization of NPs. These peaks have also been detected in other biosynthetic approaches (9,20).

#### FT-IR Analysis of AgNPs

The extracellular reduction mechanism was investigated by FT-IR spectroscopy. FT-IR analysis (Figure 3) confirmed the dual function of biological molecules through detecting the characteristic peaks in the AgNPs solution, probably due to the determining factor for the reduction and stabilization of AgNPs in the aqueous medium. In infrared spectroscopy, the energy levels of the molecules lead to oscillating chemical bonds such as the peptide bond expressing bands of amide A, B, and I-VII (21). The

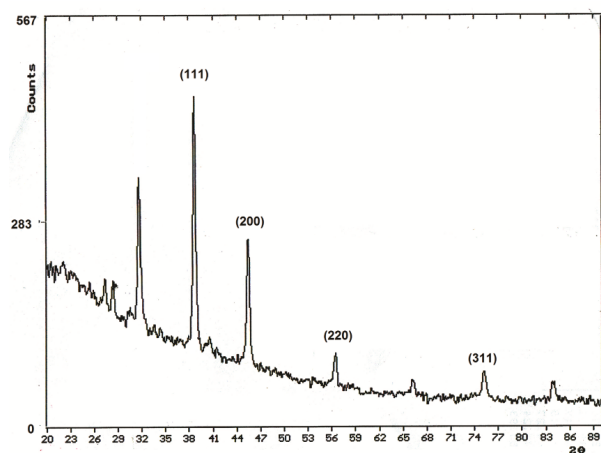


**Figure 2.** XRD Analysis of Biosynthesized AgNPs.

intense bands of amide A at  $3435\text{ cm}^{-1}$  were associated with the N-H stretching vibration of primitive and secondary amines overlapping with OH group. Amide I band at  $1637\text{ cm}^{-1}$  is mainly associated with the C=O stretching vibration. Amide II band at  $1515\text{ cm}^{-1}$  is allocated the N-H bending vibration and the C-N stretching vibration. Amides III and IV are very sophisticated bands derived from a combination of multiple correlative displacements (22). The bands at  $2924$  and  $2857\text{ cm}^{-1}$  can be associated with the symmetric and asymmetric vibrations of the Alkyne groups. The band observed at  $1741\text{ cm}^{-1}$  comes from the carboxylate group.

#### Morphology and Size Studies: SEM, EDX, and TEM

Polydispersed AgNPs were identified by SEM differing from 20 to 40 nm (Figure 4a). Biosynthesized methods can provide these types of disparities of NPs with the same size and shape (23). In addition, intense peak of Ag was identified by EDX analysis, which is obvious evidence of the formation of AgNPs (Figure 4b) (24,25). EDX pattern revealed that the paramount element is related to Ag (83.13%) in comparison with oxygen (9.84%), carbon (6.92%), and phosphorous (0.11%) (Figure 4b). Therefore, according to EDX analysis, there was an intense peak for silver, and other minor peaks were related to oxygen, carbon, and phosphorous, respectively, which were likely formed due to biomolecules linked to the surface of AgNPs (9,23).

The TEM analysis was employed to investigate the morphology and size distribution of biogenic AgNPs (Figure 4c).

As shown, polydispersed and spherical AgNPs have been formed up to a diameter of 20 nm. The edges of the particles were less weighty than the centers because of the encapsulation of the biomolecules, which resulted in the ellipticity of the particles.

#### Size Distribution and Stability of AgNPs

The DLS test demonstrated that the average size of biosynthesized AgNPs was 15.57 nm (Figure 5a). Besides, PDI verified that colloidal particles were hydrodynamically poly-dispersed at about 0.487. To investigate the subsequent

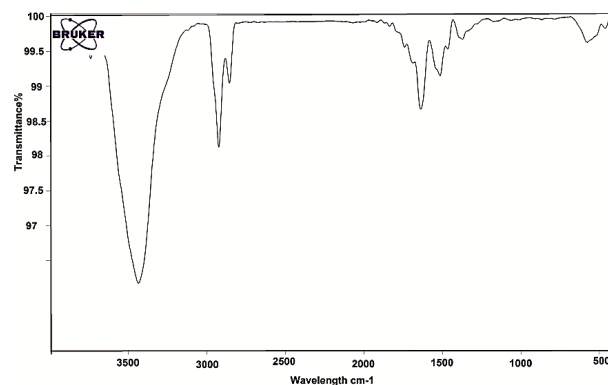


**Figure 3.** FT-IR Spectra of Biosynthesized AgNPs.

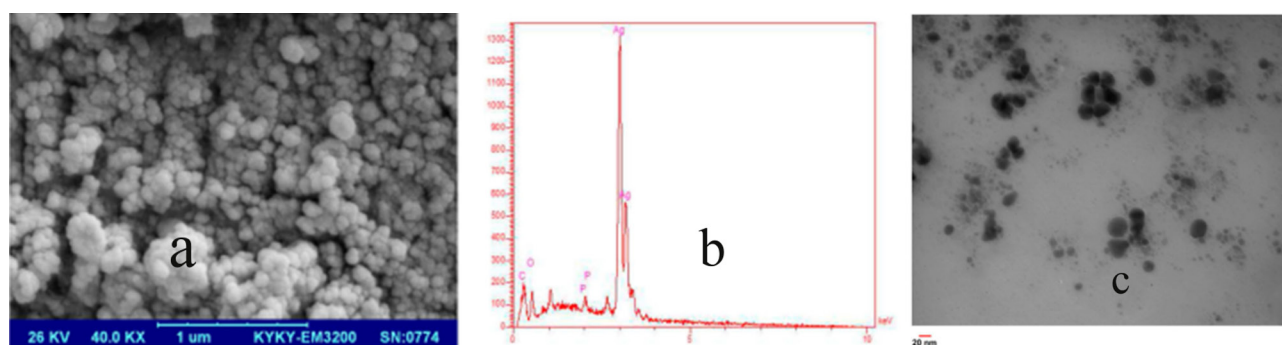


**Figure 4.** (a) SEM image of synthesized AgNPs, (b) EDX spectrum of synthesized AgNPs, and (c) TEM image of synthesized AgNPs.

interactions of the nanoparticles, the amount of surface particle charge was determined by the zeta potential. The stability of synthesized AgNPs was confirmed by negative zeta potential value of -19.2 mV (Figure 5b).

#### Antibacterial Studies of AgNPs

The in vitro antibacterial activities of silver nanoparticles against *E. coli* were significant. It was noted that increasing the concentration of  $\text{AgNO}_3$  in culture solution had an impressive role on the inhibitory activity of AgNPs (Figure 6). In the present study, zeta potential measurement confirmed the negative charge of AgNPs (Figure 5b), which can lead to attacking the gram-negative bacteria by metal depletion, as proposed by other researchers (26,27). Table 1 gives the values of inhibition zones in antibacterial studies. The inhibitory zone of biosynthesized AgNPs in 1

mM concentration of  $\text{AgNO}_3$  against *E. coli* was equal to that of gentamicin (16).

#### Discussion

In this study, we presented a new environmentally compatible and economic method for the facile biosynthesis of stable AgNPs using the sewage of a leather factory in CSL nutrient. The formation, kinetics, stability, and morphology of nanoparticles were confirmed by optical spectroscopy, as one of the most reliable techniques. A single (28) and broad SPR band peak of AgNPs is the characteristic of spherical and poly-dispersed nanoparticles (1, 29, 30). The size of the nanoparticles was determined by measuring the broadness of the peak. The more particle size increases, the narrower peak becomes with declined bandwidth and an enhanced band intensity. The maximum absorption wavelength increases with the increase of AgNPs percentage volume. Such a redshift is a characteristic of an increased nanoparticle size (1). By the increase in the reduction time of  $\text{Ag}^+$ , the intensity of absorption was strengthened for biosynthesized AgNPs and stabilized after about 6 hours of reaction. Similar results have been reported for fungal synthesized AgNPs after 96 hours (4) and 24 hours (27). None of the synthesized AgNPs showed discoloration or agglomeration during a 6-month period, suggesting its excellent stability. This stability indicates the presence of biomolecular capped onto the synthesized nano silver. A previous study reported the maximum stability duration

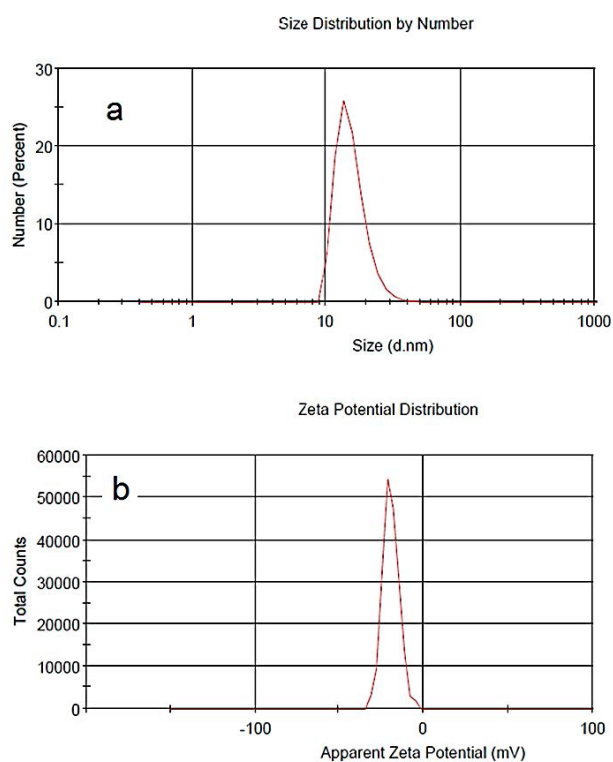


**Figure 5.** DLS of the Synthesized Silver NPs: (a) Particle size distribution, and (b) Zeta potential of synthesized AgNPs.



**Figure 6.** Zone of inhibition of silver nanoparticles against *E. coli* with various concentrations of  $\text{AgNO}_3$  (a = 0.25 mM, b = 0.5 mM and c = 1mM).

**Table 1.** Antibacterial activity of AgNPs against *E. coli* expressed in terms of the diameter of the inhibition zone

Entry	AgNO <sub>3</sub> concentration (mM)	Inhibition zone (mm)*
1	a = 0.25	8 ± 0.2
2	b = 0.5	10 ± 0.15
3	c = 1	12 ± 0.05

\* The assay was performed in triplicate.

of three months (31). FT-IR spectroscopy confirmed that the binding of proteins to NPs whether by free amines or cysteine residues in the proteins is responsible for the stabilization of extracellular nanoparticles. The overall observation confirms that the amino groups, which are related to amino acids, could reduce silver ions, and the carboxylate groups of adsorbed amino acids could cap and stabilize the synthesized AgNPs (9,32,33).

Morphological studies showed that the nanoparticles are perfectly scattered and lack any agglomeration. DLS revealed that the main reason of stability of AgNPs is likely due to the repulsive force between NPs (34). Also, previous studies revealed that there is a capping agent, which enacts an essential responsibility in keeping NPs stable (9).

The synthesized nanoparticles showed intense antibacterial activity in opposition to gram-negative bacteria. Further clinical trials are needed to study the formulation of AgNPs and treat *E. coli* cells. Considering the wide application of AgNPs, it seems essential to commercialization (mass production) biogenic AgNPs.

## Conclusions

In this study, we presented the easy biosynthesis of AgNPs using the sewage of a leather factory in CSL nutrient. The achieved results revealed that the size of synthesized AgNPs was in range of 20-40 nm and predominantly spherical, and the NPs were crystallized in the form of FCC structure. In addition, nanoparticles were perfectly scattered and lacked any agglomeration. The interaction of protein residues with Ag nanoparticles was identified, supporting that proteins play a role as both reducing and capping agents. This green and eco-compatible synthesis method, excluding the harmful reducing/capping agents, offers an amenable approach for the cost-effective production of AgNPs in large scale. The synthesized AgNPs showed antibacterial activity, providing commercial viability in biomedicine.

## Authors' Contribution

**Conceptualization:** Sirous Ebrahimi.

**Data curation:** Sirous Ebrahimi, Naeimeh Faridi Aghdam.

**Formal analysis:** Naeimeh Faridi Aghdam.

**Funding acquisition:** Shahram Moradi.

**Investigation:** Naeimeh Faridi Aghdam.

**Methodology:** Sirous Ebrahimi, Naeimeh Faridi Aghdam.

**Project administration:** Shahram Moradi.

**Resources:** Hameh Hamishehkar, Naeimeh Faridi Aghdam.

**Supervision:** Hamed Hamishehkar.

**Visualization:** Naeimeh Faridi Aghdam

**Writing—original draft:** Naeimeh Faridi Aghdam

**Writing—review & editing:** Shahram Moradi, Hamed Hamishehkar

## Conflict of Interests

Authors have no conflict of interest.

## Ethical Issues

Not applicable.

## Financial Support

We are most grateful for the financial support of this research project by the Islamic Azad University, North Tehran Branch.

## Acknowledgments

We acknowledge the support from Glucozan Co. for providing CSL and the Leather Company for providing bacterial source.

## References

- Choi O, Deng KK, Kim N-J, Ross L, Surampalli RY, Hu Z. The inhibitory effects of silver nanoparticles, silver ions, and silver chloride colloids on microbial growth. *Water Res.* 2008;42:3066-3074. doi: 10.1016/j.watres.2008.03.015
- Jha M, Shimpi NG. Green synthesis of zero valent colloidal nanosilver targeting A549 lung cancer cell: In vitro cytotoxicity. *J Genet Eng Biotechnol.* 2018;16:115-124. doi: 10.1016/j.jgeb.2018.03.001
- Azarkhalil MS, Keyvani B. Synthesis of Silver Nanoparticles from Spent X-Ray Photographic Solution via Chemical Reduction. *Iran J Chem Chem Eng (IJCCCE).* 2016;35:1-8.
- Ballottin D, Fulaz S, Cabrini F, Tsukamoto J, Durán N, Alves OL, Tasic L. Antimicrobial textiles: Biogenic silver nanoparticles against *Candida* and *Xanthomonas*. *Mater Sci Eng C.* 2017;75:582-589. doi:10.1016/j.msec.2017.02.110
- Xie W, Vu K, Yang G, Tawfiq K, Chen G. *Escherichia coli* growth and transport in the presence of nanosilver under variable growth conditions. *Environ Technol.* 2014;35:2306-2313.
- Botes M, Eugene Cloete T. The potential of nanofibers and nanobiocides in water purification. *Crit Rev Microbiol.* 2010;36:68-81.
- Hajipour MJ, Fromm KM, Ashkarran AA, de Aberasturi DJ, de Larramendi IR, Rojo T, Serpooshan V, Parak WJ, Mahmoudi M. Antibacterial properties of nanoparticles. *Trends Biotechnol.* 2012;30:499-511. doi: 10.1016/j.tibtech.2012.06.004
- Dehnavi AS, Raisi A, Aroujalian A. Control size and stability of colloidal silver nanoparticles with antibacterial activity prepared by a green synthesis method. *Synth React Inorg Met-Org Nano-Met Chem.* 2013;43:543-551. doi: 10.1080/15533174.2012.741182
- Ahila N, Ramkumar VS, Prakash S, Manikandan B, Ravindran J, Dhanalakshmi P, Kannapiran E. Synthesis of stable nanosilver particles (AgNPs) by the proteins of seagrass *Syringodium isoetifolium* and its biomedical properties. *Biomed Pharmacother.* 2016;84:60-70. doi: 10.1016/j.biopha.2016.09.004
- Abdallah BB, Landoulsi A, Chatti A. Combined static electromagnetic radiation and plant extract contribute to the biosynthesis of unstable nanosilver responsible for the growth of microstructures. *J Saudi Chem Soc.* 2018;22:110-118.
- Vijayan SR, Santhiyagu P, Ramasamy R, Arivalagan P, Kumar G, Ethiraj K, Ramaswamy BR. Seaweeds: a resource for marine bionanotechnology. *Enzyme Microb Technol.* 2016;95:45-57.
- Korbekandi H, Iravani S. Silver nanoparticles. In: *The Delivery of Nanoparticles (InTech)*; 2012.
- Nazari Z, Shafaghat A. Biological synthesis and antimicrobial

- activity of nano silver using *Hypericum scabrum* seed extract. *Inorg Nano-Met Chem*. 2017;47:870-875.
14. Yates MD, Cusick RD, Logan BE. Extracellular palladium nanoparticle production using *Geobacter sulfurreducens*. *ACS Sustainable Chem Eng*. 2013;1:1165-1171.
  15. De Corte S, Bechstein S, Lokanathan AR, Kjems J, Boon N, Meyer RL. Comparison of bacterial cells and amine-functionalized abiotic surfaces as support for Pd nanoparticle synthesis. *Colloids Surf B Biointerfaces*. 2013;102:898-904.
  16. Firdhouse MJ, Lalitha P. Biogenic silver nanoparticles–Synthesis, characterization and its potential against cancer inducing bacteria. *J Mol Liq*. 2016;222:1041-1050.
  17. Inbakandan D, Venkatesan R, Khan SA. Biosynthesis of gold nanoparticles utilizing marine sponge *Acanthella elongata* (Dendy, 1905). *Colloids Surf B Biointerfaces*. 2010;81:634-639.
  18. Velmurugan P, Iydroose M, Mohideen MHA K, Mohan TS, Cho M, Oh B-T. Biosynthesis of silver nanoparticles using *Bacillus subtilis* EWP-46 cell-free extract and evaluation of its antibacterial activity. *Bioprocess Biosyst Eng*. 2014;37:1527-1534.
  19. Vijayan SR, Santhiyagu P, Singamuthu M, Kumari Ahila N, Jayaraman R, Ethiraj K. Synthesis and characterization of silver and gold nanoparticles using aqueous extract of seaweed *Turbinaria conoides* and their antimicrofouling activity. *Sci World J*. 2014.
  20. Ibrahim HM. Green synthesis and characterization of silver nanoparticles using banana peel extract and their antimicrobial activity against representative microorganisms. *J Radiat Res Appl Sci*. 2015;8:265-275.
  21. Jabs A. Determination of Secondary Structure in Proteins by FTIR Spectroscopy. *JenyLib*; 2008 [cited 2023 Nov 8]. <https://www.jenylab.org/wp-content/uploads/2017/07/Determination-of-Secondary-Structure-in-Proteins-by-FTIR-Spectroscopy.pdf>
  22. Haris PI, Chapman D. The conformational analysis of peptides using Fourier transform IR spectroscopy. *Biopolymers*. 1995;37:251-263.
  23. Ahmad N, Sharma S, Singh V, Shamsi S, Fatma A, Mehta B. Biosynthesis of silver nanoparticles from *Desmodium triflorum*: a novel approach towards weed utilization. *Biotechnol Res Int* [Internet]. 2011 [cited 2023 Nov 8]; Available from: <https://www.hindawi.com/journals/btri/2011/454090/>
  24. Jyoti K, Baunthiyal M, Singh A. Characterization of silver nanoparticles synthesized using *Urtica dioica* Linn leaves and their synergistic effects with antibiotics. *J Radiat Res Appl Sci* [Internet]. 2016 [cited 2023 Nov 8];9:217-227.
  25. Kaviya S, Santhanalakshmi J, Viswanathan B, Muthumary J, Srinivasan K. Biosynthesis of silver nanoparticles using *Citrus sinensis* peel extract and its antibacterial activity. *Spectrochim Acta A Mol Biomol Spectrosc* [Internet]. 2011 [cited 2023 Nov 8];79:594-598.
  26. Amro NA, Kotra LP, Wadu-Mesthrige K, Bulychev A, Mobashery S, Liu G-Y. High-resolution atomic force microscopy studies of the *Escherichia coli* outer membrane: structural basis for permeability. *Langmuir*. 2000;16:2789-2796.
  27. Fayaz AM, Balaji K, Girilal M, Yadav R, Kalaichelvan PT, Venketesan R. Biogenic synthesis of silver nanoparticles and their synergistic effect with antibiotics: a study against gram-positive and gram-negative bacteria. *Nanomedicine*. 2010;6:103-109.
  28. Mie G. Beiträge zur Optik trüber Medien, speziell kolloidaler Metallösungen. *Ann Phys (Berlin, Ger)*. 1908;330:377-445.
  29. Petit C, Lixon P, Pileni MP. In situ synthesis of silver nanocluster in AOT reverse micelles. *J Phys Chem*. 1993;97:12974-12983.
  30. Kong H, Jang J. One-step fabrication of silver nanoparticle embedded polymer nanofibers by radical-mediated dispersion polymerization. *Chem Commun*. 2006;(30):3010-3012.
  31. Sathishkumar M, Sneha K, Won S, Cho C-W, Kim S, Yun Y-S. Cinnamon *zeylanicum* bark extract and powder mediated green synthesis of nano-crystalline silver particles and its bactericidal activity. *Colloids Surf B Biointerfaces*. 2009;73:332-338.
  32. Gole A, Dash C, Ramakrishnan V, Sainkar S, Mandale A, Rao M, Sastry M. Pepsin-gold colloid conjugates: preparation, characterization, and enzymatic activity. *Langmuir*. 2001;17:1674-1679.
  33. Barth A. The infrared absorption of amino acid side chains. *Prog Biophys Mol Biol*. 2000;74:141-173.
  34. Kovalchuk N, Starov V, Langston P, Hilal N. Formation of stable clusters in colloidal suspensions. *Adv Colloid Interface Sci*. 2009;147:144-154.

**Copyright** © 2024 The Author(s); This is an open-access article distributed under the terms of the Creative Commons Attribution License (<http://creativecommons.org/licenses/by/4.0>), which permits unrestricted use, distribution, and reproduction in any medium, provided the original work is properly cited.